

Single-photon nonlinear optics with Kerr-type nanostructured materials

Sara Ferretti and Dario Gerace*

Dipartimento di Fisica "Alessandro Volta," Università di Pavia, via Bassi 6, IT-27100 Pavia, Italy

(Received 2 October 2011; revised manuscript received 23 December 2011; published 10 January 2012)

We employ a quantum theory of the nonlinear optical response from an actual solid-state material possessing an intrinsic bulk contribution to the third-order nonlinear susceptibility (Kerr-type nonlinearity), which can be arbitrarily nanostructured to achieve diffraction-limited electro-magnetic-field confinement. By calculating the zero-time-delay second-order correlation of the cavity field, we set the conditions for using semiconductor or insulating materials with near-infrared energy gaps as an efficient means to obtain single-photon nonlinear behavior in prospective solid-state integrated devices, alternative to ideal sources of quantum radiation such as, e.g., single two-level emitters.

DOI: [10.1103/PhysRevB.85.033303](https://doi.org/10.1103/PhysRevB.85.033303)

PACS number(s): 42.50.Ar, 42.65.-k, 78.67.Pt

Quantum information processing based on photonic platforms is one of the most promising routes toward a fully integrated technology exploiting the laws of quantum mechanics.¹ In this context, many quantum optical tasks, such as single-photon switches and two-qubit quantum gates, would require strong photon-photon interactions—ultimately at the single-photon level—to be engineered in solid-state devices.² Besides being of practical interest for prospective applications in quantum photonics, strongly correlated photonic systems promise fascinating perspectives for a number of theoretical proposals concerning the many-body behavior of complex nonlinear and tunnel-coupled devices.^{3–5}

Cavity quantum electrodynamics (CQED) is the most straightforward way of obtaining single-photon nonlinear behavior, thanks to the underlying anharmonicity introduced by a single atomiclike emitter into a high-finesse resonator.^{6,7} It has been shown experimentally with single caesium atoms strongly coupled to a Fabry-Pérot resonant mode⁸ that such a system is able to block the transmission of a single photon when another photon is present in the cavity: a *photon blockade* effect.⁹ The quantum efficiency of this process is operationally determined by the degree of antibunching in the second-order correlation function for the emitted radiation, after resonant excitation of the CQED system.¹⁰ Analogous effects have been measured in solid-state systems with quantum dots coupled to dielectric resonators, both under nonresonant¹¹ and resonant¹² excitation conditions.

The photon blockade can be realized when two photons inside a resonant system produce a nonlinear shift of its resonance, U_{nl} , that is larger than the line broadening induced by losses and the decoherence rate, Γ , as shown in Fig. 1. Theoretical proposals to achieve single-photon nonlinearities in solid-state systems usually rely on enhanced light-matter coupling of some dipole-allowed transition, where material excitations can provide the required quantum anharmonicity. Strong Kerr-type nonlinearities are predicted for single atomiclike transitions coupled to high-quality resonators^{13,14} or in strongly confined polaritonic systems.^{15,16} For semiconductor microcavities, strong coupling of single photons mediated by enhanced second-order nonlinearity [$\chi^{(2)}$] has been theoretically discussed.¹⁷ It has also been predicted that suitably engineered coupled cavities can considerably relax the requirement on the condition that the effective nonlinear interaction be

larger than the fundamental resonance linewidth.^{18,19} However, owing to the intrinsically small value of the third-order nonlinear susceptibilities [$\chi^{(3)}$] in ordinary bulk media,²⁰ it is commonly accepted that appreciable resonance shifts for nonlinear materials in their transparency optical range would require a macroscopically large number of photons.

In this work, we challenge the latter idea by quantitatively showing that a realistic nanostructuring of an ordinary nonlinear medium is able to produce very large effective nonlinear susceptibilities, ultimately sensitive at the single-photon level. From a canonical quantization of the classical nonlinear optical response for a single mode of the electromagnetic field, we solve the quantum master equation for the system density matrix, where the real part of $\chi^{(3)}$ is related to the effective photon-photon interaction energy²¹ and losses of the resonator mode, such as coupling to free space modes or two-photon absorption, are fully taken into account.

Throughout this work, we adopt the classical nonlinear optics notation in International System (SI) units.²⁰ The nonlinear optical response to the applied electric field of a generic dielectric material is given by

$$D_i(\mathbf{r}, t) = \varepsilon_0 \varepsilon_{ij}(\mathbf{r}) E_j(\mathbf{r}, t) + \varepsilon_0 [\chi_{ijk}^{(2)}(\mathbf{r}) E_j(\mathbf{r}, t) E_k(\mathbf{r}, t) + \chi_{ijkl}^{(3)}(\mathbf{r}) E_j(\mathbf{r}, t) E_k(\mathbf{r}, t) E_l(\mathbf{r}, t) + \dots], \quad (1)$$

where we employ the usual sum rule over repeated indices labeling the three spatial coordinates. This relation defines the relative dielectric permittivity tensor of the medium, $\varepsilon_{ij}(\mathbf{r}) = \delta_{ij} + \chi_{ij}^{(1)}(\mathbf{r})$. We will now specify the nonlinear response to the case of a single mode of the electromagnetic field inside a centrosymmetric medium; i.e., we assume $\chi_{ijk}^{(2)}(\mathbf{r}) = 0$ ²⁰ and only consider Kerr-type nonlinear effects due to the $\chi^{(3)}$ tensor elements in Eq. (1). We assume an isotropic medium, i.e., a spatially dependent but scalar dielectric response, $\varepsilon_{ij}(\mathbf{r}) \rightarrow \varepsilon(\mathbf{r})$. The canonical quantization of a single mode of the electromagnetic field in a generic spatially dependent nonlinear medium is obtained after expressing the quantized field operators for a single cavity mode as

$$\hat{\mathbf{E}}(\mathbf{r}, t) = i \left(\frac{\hbar \omega_0}{2\varepsilon_0} \right)^{1/2} \left[\hat{a} \frac{\vec{\alpha}(\mathbf{r})}{\sqrt{\varepsilon(\mathbf{r})}} e^{-i\omega_0 t} - \hat{a}^\dagger \frac{\vec{\alpha}^*(\mathbf{r})}{\sqrt{\varepsilon(\mathbf{r})}} e^{i\omega_0 t} \right] \quad (2)$$

and $\hat{\mathbf{B}}(\mathbf{r}) = (-i/\omega_0) \nabla \times \hat{\mathbf{E}}(\mathbf{r})$, where \hat{a} (\hat{a}^\dagger) defines the destruction (creation) operator of a single photon in the

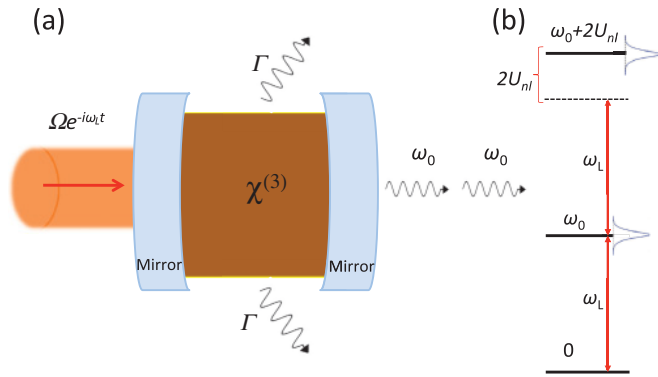


FIG. 1. (Color online) (a) Scheme of a resonator made of a Kerr-type nonlinear material, which is resonantly driven by a coherent field and undergoes a single-photon blockade. (b) Energy level diagram ($\hbar = 1$) giving rise to the emission of single-photon Fock states from the cavity.

mode and $\vec{\alpha}(\mathbf{r})$ is the normalized three-dimensional cavity field profile satisfying the condition $\int |\vec{\alpha}(\mathbf{r})|^2 d\mathbf{r} = 1$. From the classical expression of the time-averaged total-energy density in the mode, $\mathcal{H}_{em} = \frac{1}{2} \int [\mathbf{E}(\mathbf{r}) \cdot \mathbf{D}(\mathbf{r}) + \mathbf{H}(\mathbf{r}) \cdot \mathbf{B}(\mathbf{r})] d\mathbf{r}$ (assuming $\mathbf{H} = \mathbf{B}/\mu_0$ in a nonmagnetic medium), a nonlinear second-quantized Hamiltonian can be eventually obtained:

$$\hat{H} = \hbar\omega_0 \hat{a}^\dagger \hat{a} + \hat{H}_{nl}. \quad (3)$$

The linear part is the expected Hamiltonian of a single harmonic oscillator (neglecting the zero-point energy). In the nonlinear part we only retain the Kerr-type terms,²² $\hat{H}_{nl} = U_{nl} \hat{a}^\dagger \hat{a}^\dagger \hat{a} \hat{a}$, with the photon-photon interaction given by

$$U_{nl} = \frac{D(\hbar\omega_0)^2}{8\epsilon_0} \int d\mathbf{r} \alpha_i^*(\mathbf{r}) \frac{\text{Re}\{\chi_{ijkl}^{(3)}(\mathbf{r})\}}{\epsilon^2(\mathbf{r})} \alpha_j^*(\mathbf{r}) \alpha_k(\mathbf{r}) \alpha_l(\mathbf{r}), \quad (4)$$

with degeneracy $D = 6$. Equation (4) is a general expression for the nonlinear shift induced by the Kerr effect at the single-photon level, for an arbitrary spatially modulated field confinement, such as photonic crystal or pillar microcavities made of ordinary nonlinear semiconductor materials.²³ Even if the full expression should be applied to the specific case of interest for given nonlinear tensor components, we can simplify Eq. (4) to give some quantitative estimates:²⁴

$$U_{nl} \simeq \frac{3(\hbar\omega_0)^2}{4\epsilon_0} \frac{\bar{\chi}^{(3)}}{\bar{\epsilon}_r^2} \int |\vec{\alpha}(\mathbf{r})|^4 d\mathbf{r} = \frac{3(\hbar\omega_0)^2}{4\epsilon_0 V_{\text{eff}}} \frac{\bar{\chi}^{(3)}}{\bar{\epsilon}_r^2}, \quad (5)$$

where the effective cavity mode volume is defined as $V_{\text{eff}}^{-1} = \int |\vec{\alpha}(\mathbf{r})|^4 d\mathbf{r}$ within our formalism. To have order-of-magnitude results, we assume constant values for the average real part of the nonlinear susceptibility and relative dielectric permittivity, $\bar{\chi}^{(3)}$ and $\bar{\epsilon}_r$, respectively. We neglect self-consistent nonlinear effects on the cavity field profile induced by the Kerr nonlinearity itself (e.g., field expulsion from the cavity region), which could renormalize the effective value of U_{nl} .

The experimental configuration for the photon blockade can be modeled by adding a coherent pumping term to obtain

the standard Kerr-type Hamiltonian that is usually employed in quantum optics:²⁴

$$\hat{H} = \hbar\omega_0 \hat{a}^\dagger \hat{a} + U_{nl} \hat{a}^\dagger \hat{a}^\dagger \hat{a} \hat{a} + F e^{-i\omega_L t} \hat{a}^\dagger + F^* e^{i\omega_L t} \hat{a}, \quad (6)$$

where $\Omega = F/\hbar$ is the coherent pumping rate at the laser frequency ω_L . Losses in the system are quantified either through the intrinsic cavity decay rate, κ , or nonlinear absorption processes, such as the two-photon absorption (TPA) rate, γ_{TPA} . The first is due to coupling of the resonant mode to free space modes, material absorption, or scattering from roughness, and defines the cavity quality (Q) factor as $Q = \omega_0/\kappa$; the latter is related to the imaginary part of the nonlinear susceptibility. Such loss mechanisms are taken into account within a density-matrix master-equation formalism in Markov approximation:

$$\dot{\rho} = \frac{i}{\hbar} [\rho, \hat{H}] + \mathcal{L}_1(\kappa, \rho) + \mathcal{L}_2(\gamma_{\text{TPA}}, \rho), \quad (7)$$

where $\mathcal{L}_1 = \kappa[\hat{a}\rho\hat{a}^\dagger - \hat{a}^\dagger\hat{a}\rho/2 - \rho\hat{a}^\dagger\hat{a}/2]$ and $\mathcal{L}_2 = \gamma_{\text{TPA}}[\hat{a}^2\rho(\hat{a}^\dagger)^2 - (\hat{a}^\dagger)^2\hat{a}^2\rho/2 - \rho(\hat{a}^\dagger)^2\hat{a}^2/2]$ are the linear and nonlinear Liouvillian operators, respectively. In classical nonlinear optics, TPA is quantitatively defined by an intensity-dependent absorption coefficient, $\alpha_{\text{TPA}} = \beta I$, where β is measured in m/W and is well known for many semiconductor or insulator materials.²⁰ Such a quantity is related to a loss rate, $\gamma_{\text{TPA}} = \beta c I / 2\bar{n}_r$, where $\bar{n}_r^2 = \bar{\epsilon}_r$ and I is the field intensity in the cavity.²⁵

The figure of merit (FOM) quantifying the single-photon nonlinear behavior of the cavity mode is the normalized zero-time-delay second-order correlation, defined as $g^{(2)}(0) = \langle \hat{a}^{\dagger 2} \hat{a}^2 \rangle / \langle \hat{a}^\dagger \hat{a} \rangle^2$. Single photons are released from the cavity at the bare frequency, ω_0 . In the weak resonant excitation limit ($\Omega/\kappa \ll 1$) a closed analytic solution for the model considered is found after truncating the Hilbert space to the $n = 2$ Fock state:⁵

$$g^{(2)}(0) = \frac{1 + 4(\Delta E/\hbar\kappa)^2}{1 + 4(\Delta E + U_{nl})^2/\hbar^2\kappa^2}, \quad (8)$$

where $\Delta E = \hbar(\omega_L - \omega_0) = \hbar\Delta\omega$. For $g^{(2)}(0) \rightarrow 0$ we have an almost ideal single-photon source,²¹ which occurs when $U_{nl}/(\hbar\kappa) \gg 1$. From Eqs. (5) and (8), $\text{FOM} = Q^2/V_{\text{eff}}^2$ is the relevant figure of merit to be optimized.

The steady-state value of $g^{(2)}(0)$ can also be calculated numerically through a quantum average on ρ_{ss} , which is the density matrix corresponding to the eigenvalue $\lambda_{\text{ss}} = 0$ in the linear eigenvalue problem $\mathcal{L}\rho = \lambda\rho$.²⁶ Convergence is ensured by truncating the Hilbert space to a large number of photons (up to 50 in this work). A close agreement between analytic and numerical solutions is reported in Fig. 2, where we show $g^{(2)}(0)$ in the low-pumping regime as a function of the confinement volume and pump/cavity detuning, respectively. Results are plotted for different values of the ratio $\bar{\chi}^{(3)}/\bar{\epsilon}_r^2$, which is a material-dependent quantity. We assume an operational energy, $\hbar\omega_0 = 1$ eV, as representative of typical near-infrared applications, and a realistic quality factor $Q = 10^6$ (see discussion below). As shown in Fig. 2(a), for $V_{\text{eff}} \ll \lambda_0^3$ the system exhibits a strong antibunching, which is the signature of single-photon blockade. For materials with larger $\bar{\chi}^{(3)}/\bar{\epsilon}_r^2$ ratios, the condition for achieving nonlinear behavior at the

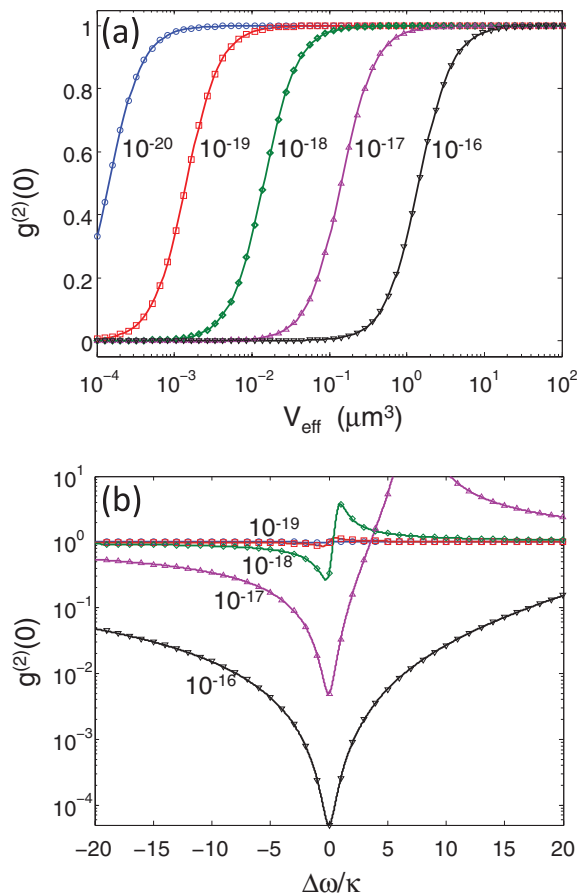


FIG. 2. (Color online) Numerical (symbols) and analytic (full lines) solutions for the zero-time-delay second-order correlation for different $\bar{\chi}^{(3)}/\bar{\epsilon}_r^2$ values. (a) Dependence on effective confinement volume of the cavity field with parameters $\hbar\omega_0 = 1$ eV, $\Delta\omega = 0$, and $Q = 10^6$. (b) Dependence on the detuning between the driving field and cavity resonance, for $V_{\text{eff}} = 0.01 \mu\text{m}^3$ and parameters as before. Numerical results are calculated with $\Omega/\kappa = 0.01$.

single-photon level is quantitatively relaxed, making it possible to observe strong antibunching even for $V_{\text{eff}} \sim \lambda_0^3$. Figure 2(a) emerges then as a useful road map to quantitatively assess, for a specific nanostructured material, the combined effect of third-order susceptibility and the confinement volume on getting a nonlinear response at the single-photon level. A realistic value $V_{\text{eff}} = 0.01 \mu\text{m}^3$ can be assumed for diffraction-limited confinement volumes, i.e., $V_{\text{eff}} \sim (\lambda_0/2\bar{n}_r)^3$, where \bar{n}_r can display values between 2 and 4, depending on the semiconductor or insulator material under investigation.²⁰ In Fig. 2(b), we show $g^{(2)}(0)$ as a function of pump/cavity detuning and a fixed value of the confinement volume. At a large $\bar{\chi}^{(3)}/\bar{\epsilon}_r^2$ ratio, the maximum antibunching is obtained for $\Delta\omega \sim 0$. At positive detunings, the bunching is due to the driving laser hitting the two-photon resonance of the cavity [see the scheme in Fig. 1(b)].¹⁵ Again, in this low-pumping regime the quantitative behavior of $g^{(2)}(0)$ obtained from the numerical solution is closely reproduced analytically.

The results shown in Fig. 2 may represent a useful guide to quantum photonics experiments employing ordinary nonlinear materials, whose relevant figure of merit for single-photon nonlinear behavior can be predicted for any specific

TABLE I. Third-order nonlinear optical coefficients of different semiconductor and doped glass materials at specific wavelengths in the near infrared.

Material	$\text{Re}\{\chi^{(3)}\}$ (m^2/V^2)	β (m/W)	n_r	λ (μm)
Si ²⁷⁻²⁹	0.45×10^{-18}	10^{-11}	3.4	1.55
Ge ²⁹	4×10^{-18}	10^{-8}	4.0	2.5
GaAs ²⁷	0.6×10^{-18}	10^{-10}	3.4	1.54
SiO ₂ /Ge ³⁰	1.4×10^{-18}	4×10^{-10}	2	0.8
SiO ₂ /Si-nc ³¹	2.1×10^{-18}	5×10^{-10}	1.74	1.55
SiO ₂ /Ag ³²	7×10^{-16}	1.5×10^{-11}	1.8	1.06

nanostructuring-based confinement. For example, diffraction-limited electro-magnetic-field confinement can be achieved by using photonic crystal nanocavities, in which a number of remarkable figures of merit have been already demonstrated experimentally (for a recent review, see Ref. 33). Quite interestingly and related to the present work, most of such achievements have been obtained by using highly nonlinear materials, such as silicon (Si) or gallium arsenide (GaAs). The typical order of magnitude for the $\chi^{(3)}$ tensor elements of these materials is in the range $\text{Re}\{\chi^{(3)}\} \sim 10^{-19} - 10^{-18} \text{ m}^2/\text{V}^2$.²⁰ However, even larger $\chi^{(3)}$ values can be found in certain glasses doped with nanoparticles, chalcogenide glasses, or other polymeric materials.²⁰ We refer to Table I for a few recent experimental references on the nonlinear coefficients of some Kerr-type materials in the near infrared, which we have collected from published works and converted in SI units. Most of these materials can be nanostructured to fabricate solid-state nanocavities. Ultra-high- Q factors in excess of 10^6 have been experimentally shown, corresponding to a photon lifetime within the cavity region on the order of one to few ns, and 10^8 has been predicted through design optimization.³³ Designs to achieve sub-diffraction-limited mode volumes, on the order of $V_{\text{eff}} \sim (\lambda/2n_r)^3$, have been also proposed.³⁴ Further reduction of the confinement volume, well below the diffraction limit, has been predicted for suitably engineered nanostructures.³⁵ Thanks to these unprecedented figures of merit, strong enhancement of the nonlinear optical response due to $\chi^{(3)}$ nonlinearity has been already shown in GaAs- and Si-based photonic crystal cavities around $\lambda \sim 1.5 \mu\text{m}$, respectively.³⁶

To quantitatively assess the role of TPA on the $g^{(2)}(0)$ as a function of the pumping strength, we have numerically calculated this figure of merit for realistic values of the nonlinear coefficients. We assume a simple normalized mode profile $\alpha(\bar{r}) = N \exp(-x^2/2\sigma_x^2 - y^2/2\sigma_y^2) \cos(\pi/d)z$, where the normalization factor $N = (2/\pi\sigma_x\sigma_y d)^{1/2}$. This functional form is a good approximation for a photonic crystal confinement in the (x, y) plane (Gaussian envelope function) and index confinement in the transverse direction, such as the one that can be obtained with a point defect in a triangular lattice on a planar membrane of thickness d .³³ From our definition of effective mode volume we have $V_{\text{eff}} = 4\pi\sigma_x\sigma_y d/3$. As illustrative examples, we show results in Fig. 3 for two different Kerr-type materials. In Fig. 3(a) we assume a high-index ($n_r \sim 3.4$) and strongly nonlinear medium, with a typical TPA coefficient in the telecom band.²⁰ In such a case, we can assume realistic confinement lengths on the order of

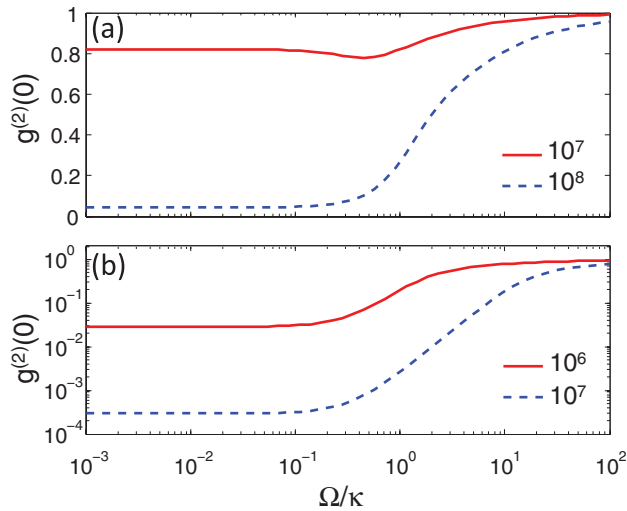


FIG. 3. (Color online) Single-photon nonlinear behavior as a function of the driving strength for a nanocavity made of (a) a high-index Kerr-type medium with $\text{Re}\{\chi^{(3)}\} = 10^{-18} \text{ m}^2/\text{V}^2$, $\bar{\epsilon}_r = 10$, $\beta = 10^{-10} \text{ m/W}$, and $V_{\text{eff}} = 10^{-3} \mu\text{m}^3$ or (b) a low-index, strongly nonlinear material with $\text{Re}\{\chi^{(3)}\} = 10^{-16} \text{ m}^2/\text{V}^2$, $\bar{\epsilon}_r = 4$, $\beta = 10^{-11} \text{ m/W}$, and $V_{\text{eff}} = 10^{-2} \mu\text{m}^3$. In both cases, $\hbar\omega_0 = 0.8 \text{ eV}$ ($\lambda_0 = 1.55 \mu\text{m}$). The results are shown for (a) $Q = 10^7$ (full line) and $Q = 10^8$ (dashed line) and (b) $Q = 10^6$ (full line) and $Q = 10^7$ (dashed line).

$\sigma_{x,y} \simeq \lambda_0/(4n_r)$ and $d = \lambda_0/(2n_r)$, which gives an optimistic $V_{\text{eff}} \simeq 0.001 \mu\text{m}^3$ for wavelengths on the order of $\lambda_0 = 1 \mu\text{m}$. In Fig. 3(b) we assume a low-index ($n_r \sim 2$) material with a sizable Kerr nonlinearity and negligible TPA coefficient at telecom wavelengths (such as silica with metal nanoparticles; see Table I). In such a case, the confinement lengths can be $\sigma_x \simeq \lambda_0/(2n_r)$, $\sigma_y \simeq \lambda_0/(10n_r)$, and $d = \lambda_0/(2n_r)$, where one exploits the slot waveguide confinement at least along one direction.³⁵ With these numbers at hand, we can again assume $V_{\text{eff}} \simeq 0.01 \mu\text{m}^3$ for this case. These results clearly show that efficient single-photon nonlinear behavior can be achieved with ordinary Kerr-type media and that such behavior is robust with respect to nonlinear sources of dissipation such as TPA. In particular, we notice that in Fig. 3(a) TPA contributes a nonlinear quality factor $Q_{\text{TPA}} \simeq 10^8$ for $\Omega/\kappa \simeq 10^2$, which means that its effects become relevant only for strong pumping strength and very large $\omega_0/\kappa \sim 10^8$. Realistic Q factors on the order of 10^7 can already give clear signatures of single-photon nonlinear behavior and sizable antibunching with such high-index media. On the other hand, the stronger nonlinearity of doped glasses, together with their negligible TPA effects at telecom wavelengths, make these materials extremely interesting for quantum photonics

applications. From Fig. 3(b), Q factors on the order of 10^6 are already sufficient to give an almost ideal single-photon source, provided the confinement volume is as low as the one assumed.

So far, we have assumed continuous wave excitation, i.e., $\Omega \neq \Omega(t)$. Common solid-state single-photon sources exploit the reduced lifetime of a quantum emitter in a cavity, allowing single-photon generation on demand at high repetition rates through pulsed excitation.¹ A single-photon source based on the simple scheme of Fig. 1 has the potential advantage of working at arbitrary wavelengths (determined by the cavity resonance), with a radiative time scale solely determined by the cavity mode characteristic parameters, thanks to the basically instantaneous nature of $\chi^{(3)}$ processes.²⁰ Thus, in a pulsed excitation scheme the requirements on the resonant laser source are determined by the constraints on the pulse duration ($\hbar/U_{\text{nl}} < \Delta t < \kappa^{-1}$) and period ($\Delta T \geq 5\kappa^{-1}$) preserving the photon blockade.^{9,15} From the results shown in Fig. 2(b), the device would also be tolerant to possible fluctuations of the laser center frequency around the cavity resonance, which are normally smaller than the cavity linewidth in standard near-infrared laser sources. With a $Q \simeq 10^6$, i.e., $\kappa^{-1} \sim 1 \text{ ns}$, and U_{nl} of a few μeV , the pulse duration should be between 0.1 and 1 ns, while the maximum repetition rate would be limited to a few hundred MHz, which is comparable to the fastest single-photon source on demand recently demonstrated with solid-state quantum emitters.³⁷ The potential repetition rate can be further increased by relaxing the requirements on the Q factor, i.e., by increasing U_{nl} through reduction of the cavity mode volume, anticipating much more controllability and flexibility as compared to single quantum emitters.

In summary, we have shown that future quantum photonics applications can strongly benefit from the capability of nanostructuring ordinary Kerr-type materials to achieve sub-diffraction-limited electro-magnetic-field confinement. The growing interest in integrated quantum photonics,³⁸ and the possibility of fully exploiting the mature complementary metal-oxide semiconductor-based technology to build room-temperature and intrinsically flexible single-photon devices is likely to produce new research avenues based on the present proposal in the near future.

We acknowledge several useful and motivating discussions with L. C. Andreani, D. Bajoni, I. Carusotto, M. Galli, M. Liscidini, L. O'Faolain, V. Savona, and H. E. Türeci. This work is partly supported from the Italian Ministry of University and Research through Fondo Investimenti Ricerca di Base (FIRB) Contract No. RBF08QIP5 and from project NanoSci-ERANET project "Leccsin." Support from the foundation Alma Mater Ticinensis is acknowledged.

*dario.gerace@unipv.it.

¹J. L. O'Brien *et al.*, *Nat. Photonics* **3**, 687 (2009).

²A. Imamoglu, D. D. Awschalom, G. Burkard, D. P. DiVincenzo, D. Loss, M. Sherwin, and A. Small, *Phys. Rev. Lett.* **83**, 4204 (1999).

³M. J. Hartmann *et al.*, *Nat. Physics* **2**, 849 (2006); A. D. Greentree *et al.*, *ibid.* **2**, 856 (2006); D. G. Angelakis, M. F. Santos, and

S. Bose, *Phys. Rev. A* **76**, 031805(R) (2007); D. Rossini and R. Fazio, *Phys. Rev. Lett.* **99**, 186401 (2007).

⁴D. Gerace *et al.*, *Nat. Physics* **5**, 281 (2009); I. Carusotto, D. Gerace, H. E. Türeci, S. DeLiberato, C. Ciuti, and A. Imamoglu, *Phys. Rev. Lett.* **103**, 033601 (2009).

⁵S. Ferretti, L. C. Andreani, H. E. Türeci, and D. Gerace, *Phys. Rev. A* **82**, 013841 (2010).

- ⁶L. Tian and H. J. Carmichael, *Phys. Rev. A* **46**, 6801(R) (1992).
- ⁷M. J. Werner and A. Imamoğlu, *Phys. Rev. A* **61**, 011801(R) (1999).
- ⁸K. M. Birnbaum *et al.*, *Nature (London)* **436**, 87 (2005).
- ⁹A. Imamoğlu, H. Schmidt, G. Woods, and M. Deutsch, *Phys. Rev. Lett.* **79**, 1467 (1997).
- ¹⁰S. Rebić, A. S. Parkins, and S. M. Tan, *Phys. Rev. A* **69**, 035804 (2004).
- ¹¹K. Hennessy *et al.*, *Nature (London)* **445**, 896 (2007); D. Press, S. Gotzinger, S. Reitzenstein, C. Hofmann, A. Löffler, M. Kamp, A. Forchel, and Y. Yamamoto, *Phys. Rev. Lett.* **98**, 117402 (2007).
- ¹²A. Faraon *et al.*, *Nat. Physics* **4**, 859 (2008).
- ¹³A. Auffèves-Garnier, C. Simon, J. M. Gerard, and J. P. Poizat, *Phys. Rev. A* **75**, 053823 (2007).
- ¹⁴K. Jacobs and A. J. Landahl, *Phys. Rev. Lett.* **103**, 067201 (2009).
- ¹⁵A. Verger, C. Ciuti, and I. Carusotto, *Phys. Rev. B* **73**, 193306 (2006).
- ¹⁶I. Carusotto *et al.*, *Europhys. Lett.* **90**, 37001 (2010).
- ¹⁷W. T. M. Irvine, K. Hennessy, and D. Bouwmeester, *Phys. Rev. Lett.* **96**, 057405 (2006).
- ¹⁸T. C. H. Liew and V. Savona, *Phys. Rev. Lett.* **104**, 183601 (2010).
- ¹⁹M. Bamba, A. Imamoğlu, I. Carusotto, and C. Ciuti, *Phys. Rev. A* **83**, 021802(R) (2011).
- ²⁰R. W. Boyd, *Nonlinear Optics* (Academic Press, New York, 2008).
- ²¹R. Loudon, *The Quantum Theory of Light* (Clarendon Press, Oxford, 1983).
- ²²J. E. Sipe, N. A. R. Bhat, P. Chak, and S. Pereira, *Phys. Rev. E* **69**, 016604 (2004).
- ²³K. J. Vahala, *Nature (London)* **424**, 839 (2003).
- ²⁴P. D. Drummond and D. F. Walls, *J. Phys. A* **13**, 725 (1980).
- ²⁵The absorption coefficient is related to the imaginary part of the frequency (and hence to the loss rate) as $\alpha_{\text{TPA}} = 2\text{Im}(\omega)n_r/c$, where n_r is the material refractive index and c is the speed of light.
- ²⁶M. Jakob and S. Stenholm, *Phys. Rev. A* **67**, 032111 (2003).
- ²⁷M. Dinu *et al.*, *Appl. Phys. Lett.* **82**, 2954 (2003).
- ²⁸A. D. Bristow *et al.*, *Appl. Phys. Lett.* **90**, 191104 (2007).
- ²⁹N. K. Hon *et al.*, *J. Appl. Phys.* **110**, 011301 (2011).
- ³⁰L. Razzari *et al.*, *Appl. Phys. Lett.* **88**, 181901 (2006).
- ³¹A. Martinez *et al.*, *Nano Lett.* **10**, 1506 (2010).
- ³²R. A. Ganeev and A. I. Ryasnyansky, *Appl. Phys. B* **84**, 295 (2006).
- ³³M. Notomi, *Rep. Prog. Phys.* **73**, 096501 (2010).
- ³⁴S. Nakayama *et al.*, *Appl. Phys. Lett.* **98**, 171102 (2011).
- ³⁵J. T. Robinson, C. Manolatu, L. Chen, and M. Lipson, *Phys. Rev. Lett.* **95**, 143901 (2005).
- ³⁶S. Combrié *et al.*, *Opt. Lett.* **33**, 1908 (2008); M. Galli *et al.*, *Opt. Express* **18**, 26613 (2010).
- ³⁷K. Rivoire *et al.*, *Appl. Phys. Lett.* **98**, 083105 (2011).
- ³⁸A. Politi *et al.*, *Science* **320**, 646 (2008); **325**, 1221 (2009).